JACS
JOURNAL OF THE AMERICAN CHEMICAL SOCIETY
Article
pubs.acs.org/JACS

Single Molecule Force Spectroscopy Reveals the Molecular Mechanical Anisotropy of the FeS_4 Metal Center in Rubredoxin

Peng Zheng,[†] Chih-Chung Chou,[†] Ying Guo,[†] Yanyan Wang,[†,‡] and Hongbin Li*[,†,‡]

[†]Department of Chemistry, University of British Columbia Vancouver, British Columbia V6T 1Z1, Canada

[‡]State Key Laboratory of Precision Measurements Technology and Instruments, School of Precision Instrument and Opto-Electronics Engineering, Tianjin University, Tianjin, 30072 P. R. China

Supporting Information

ABSTRACT: Mechanical anisotropy is an important feature of materials. Depending on the direction it is pulled, a material can exhibit very different mechanical properties. Mechanical anisotropy on the microscopic scale has also been observed for individual elastomeric proteins. Depending upon the direction along which it is stretched, a protein can unfold via different mechanical unfolding pathways and exhibit vastly different mechanical stability. However, it remains to be demonstrated if the concept of mechanical anisotropy can be extended to the molecular scale for small molecular objects containing only a few chemical bonds. Here, we choose the iron−sulfur center FeS_4 in the simplest iron−sulfur protein rubredoxin as a model system to demonstrate the molecular level mechanical anisotropy. We used single molecule atomic force spectroscopy to investigate the mechanical rupture of the FeS_4 center along different pulling directions. The FeS_4 cluster is a simple molecular object with defined three-dimensional structure, where a ferric ion and four coordinating cysteinyl ligands are arranged into a distorted tetrahedral geometry. Mutating two specific residues in rubredoxin to cysteines provides anchoring points that enable us to stretch and rupture the FeS_4 center along five distinct and precisely controlled directions. Our results showed that the mechanical stability as well as the rupture mechanism and kinetics of the FeS_4 center are strongly dependent upon the direction along which it is stretched, suggesting that the very small and simple FeS_4 center exhibits considerable mechanical anisotropy. It is likely that structural asymmetry in the FeS_4 cluster and the modulation of the local environment due to partial unfolding of rubredoxin are responsible for the observed mechanical anisotropy. Our results suggest that mechanical anisotropy is a universal feature for any asymmetrical three-dimensional structure, even down to a molecular scale, and such mechanical anisotropy can be potentially utilized to control the mechanochemical reactivity of molecular objects.

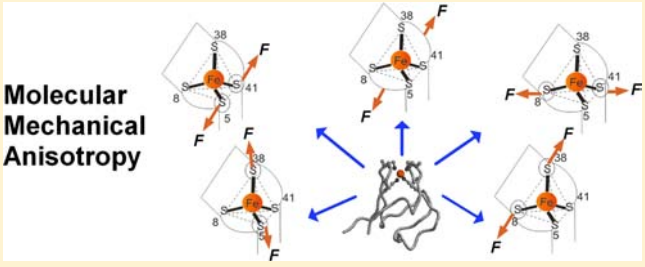

INTRODUCTION

Due to structural anisotropy, mechanical properties of macroscopic materials often exhibit anisotropy, where a material can exhibit vastly different mechanical properties depending on the direction in which it is pulled, which in turn determines the specific applications of these materials.[1,2] Graphite is a well-known case of anisotropy, showing a vastly different stability when stretched along the direction that is parallel or perpendicular to its molecular ring structure. Over the past decade, the development of single molecule force spectroscopy techniques has made it possible to study mechanical anisotropy on the microscopic scale on individual elastomeric proteins.[3−10] Such mechanical anisotropy on the microscopic scale was first observed on a small all-β protein E2lip3[6] and a small α/β protein ubiquitin,[3] and later in many other proteins.[4,5,7,8,10−12] By selecting two well-defined residues, a protein can be stretched along different directions in single molecule force spectroscopy experiments. In these experiments, the pulling direction is determined by the two anchoring points, and the protein chain (including folded and unfolded sequences) serves as a rope to deliver the force to the protein via the two anchoring points. As a consequence, a protein can unfold along different pathways and exhibits different mechanical stability depending on the direction along which it is stretched.[3−5,10,12,13] Molecular dynamics simulations corroborated such mechanical anisotropy and revealed that the molecular origin of mechanical anisotropy lies in different interactions that are to be ruptured as the protein is stretched along different pulling directions.[3,5−7,10] These results provide a reliable means to manipulate single protein along different directions using single molecule force spectroscopy techniques. Although microscopic mechanical anisotropy is observed in individual proteins, hundreds of chemical bonds and non-covalent interactions are involved during the mechanical unfolding process, even for small proteins with <100 amino acid residues. It remains to be established whether mechanical anisotropy can be observed on the molecular scale for small molecular objects containing only a few chemical bonds, such as metal clusters.[14,15] Moreover, it is yet to be demonstrated

Received: July 1, 2013
Published: October 30, 2013

   dx.doi.org/10.1021/ja406695g | J. Am. Chem. Soc. 2013, 135, 17783−17792

how a stretching force can be applied to small molecular objects along distinct and well-controlled directions due to the size of such small molecular objects. To address these questions, we have combined single molecule atomic force microscopy (AFM) and protein engineering techniques to investigate how a naturally occurring metal cluster responds to mechanical stretching forces that are applied in several distinct and precisely controlled directions.

The FeS_4 metal center in the simplest iron–sulfur protein *Pyrococcus furiosus* rubredoxin (*pf*-RD) was chosen as the experimental subject due to its small size and structural simplicity.[16−18] Metal cluster FeS_4 occurs naturally in rubredoxins, and its inorganic analogues have also been previously synthesized.[19−21] The FeS_4 cluster is a simple molecular object with defined three-dimensional (3D) structure, where a ferric ion is coordinated by four cysteinyl ligands arranged into a tetrahedral geometry (Figure 1A).[22]

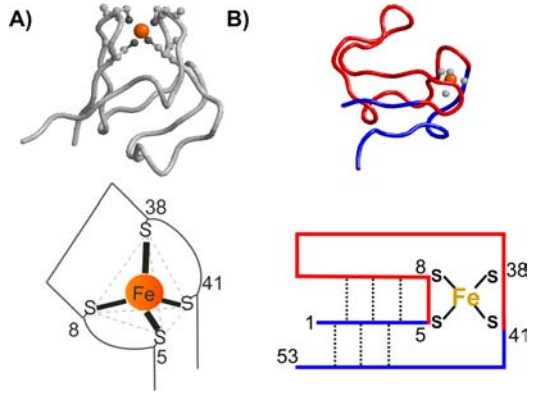

Figure 1. Details of the rubredoxin structure. (A) The 3D structure of rubredoxin, which contains a FeS_4 center where a ferric ion is coordinated by four sulfur atoms from cysteine residues. The bottom is a schematic of rubredoxin with the tetrahedron FeS_4 center highlighted. (B) The side-view of rubredoxin. The bottom is a simple line drawing schematic showing the overall structure of rubredoxin. Dotted lines indicate the backbone hydrogen bonds connecting β-strands. Residues that are outside the FeS_4 center are colored in blue, while residues that are sequestered by the FeS_4 center are colored in red.

Depending on how force is applied to this geometry, the FeS_4 cluster can be stretched along a maximum of six distinct pulling directions, thus offering an ideal model system to study potential molecular level mechanical anisotropy.

For the FeS_4 cluster in rubredoxin, two CXXC chelation loops coordinate the ferric ion by forming four ferric–thiolate bonds (for simplicity, these ferric–thiolate bonds are abbreviated as Fe–S(Cys5); Fe–S(Cys8); Fe–S(Cys38); and Fe–S(Cys41) bond in this study), and the center itself assumes a pseudotetrahedral geometry. The FeS_4 center divides rubredoxin into two parts: residues 1–4 and 42–53 are outside the center, while residues 5–41 are trapped inside the center (Figure 1B). In our previous work, we have shown that it is possible to mechanically unfold rubredoxin and rupture the FeS_4 center using the AFM by stretching the wild-type rubredoxin along its N- and C-termini.[17,18,23] In this pulling geometry, after structural elements outside of the FeS_4 center have been unfolded, the stretching force will be applied to the FeS_4 center along the direction defined by Cys5 and Cys41. These observations have been validated recently by quantum mechanics/molecular dynamics calculations of the mechanical unfolding of rubredoxin and the rupture of FeS_4 center.[24] In this study, we will investigate how the FeS_4 center responds to the stretching force that is applied to the center along different pulling directions. Although the FeS_4 center is the subject of interest in this study, the protein framework surrounding the metal center is also critical for discerning the mechanical response of FeS_4 when stretched along different directions. On the one hand, rubredoxin framework provides an indispensable handle to apply force to the FeS_4 center. On the other hand, the unique contour length increment from the partial unfolding of rubredoxin and the rupture of metal center under different pulling direction provide an unambiguous signature to validate our designed pulling direction on the FeS_4 center of rubredoxin.

METHODS AND MATERIALS

Protein Engineering. The genes encoding bicysteine variants RD1,49, RD15,49, RD15,35, RD1,35 and RD6,40 were engineered using standard site-directed mutagenesis methods based on wild-type rubredoxin gene. The numbers in each variant indicate the residues that are mutated to cysteines. The two cysteine substitutions were introduced into the rubredoxin gene in two sequential steps. DNA sequences were confirmed by DNA sequencing. All proteins were overexpressed in the DH5α strain of *E. coli* and purified by Co^{2+}-affinity chromatography using TALON His-Tag purification resins (Clontech.). Using a 3K MWCO Amicon ultra centrifugal filter (Millipore), the protein solution was exchanged into Tris buffer (pH 8.5, 10 mM). The Fe form rubredoxin variants were then separated using ion exchange chromatography. Finally, polyproteins were obtained using a thiol-maleimide coupling reaction between the cysteines of rubredoxin and $BM(PEO)_3$.[17] All the rubredoxin mutants show characteristic UV–vis spectra that are comparable to that of wild-type rubredoxin.

Single Molecule AFM Experiments. A custom-built AFM as described previously[25] was used for all single-molecule AFM experiments reported here. The spring constant (typically around 40 pN/nm) of each Si_3N_4 cantilever (MLCT probe, Bruker Corp.) was obtained in solution using the equipartition theorem[26] before each experiment. Data acquisition and analysis were done using custom-written codes in Igor Pro (Wavemetrics, Lake Oswego).

Single molecule AFM experiments were performed following well-established method.[27−32] In a typical experiment, ~2 μL of the polyprotein solution at a concentration of ~2 mg/mL was added to a clean glass coverslip covered by ~50 μL of Tris buffer (pH ~7.5). The protein was allowed to absorb for ~5 min before force–extension measurements. During AFM experiments, the cantilever was brought into contact with the substrate at a contact force of ~1 nN and then retracted away from the surface to pick up and stretch polyprotein molecules. A typical pulling speed used in our force–extension measurements is 400 nm/s. On average, about 2% of trials lead to the picking up and stretching of single polyprotein molecules.

Individual force peaks in the sawtooth-like force–extension curves were fitted using the worm-like chain (WLC) model of polymer elasticity[33] to measure the contour length increment upon domain unfolding and the rupture of FeS_4 center. The persistence length used in the WLC fitting is ~0.4 nm, which is typical for polyproteins with a long spacer or unfolded domains.[6,11,34,35]

Monte Carlo Simulations. The mechanical rupture process of the FeS_4 center can be modeled as a two-state rupture process with force-dependent rate constants:[36−38]

$$k_r(F) = k_{r0} \times \exp\left(\frac{F \cdot \Delta x}{k_B T}\right) \quad (1)$$

where $k_r(F)$ is the rate constant for dissociation at a stretching force F, k_{r0} is the spontaneous dissociation rate constant at zero force, Δx is the distance between the bound and transition states, k_B is the Boltzmann constant, and T is the absolute temperature. Since the force–extension

dx.doi.org/10.1021/ja406695g | J. Am. Chem. Soc. 2013, 135, 17783−17792

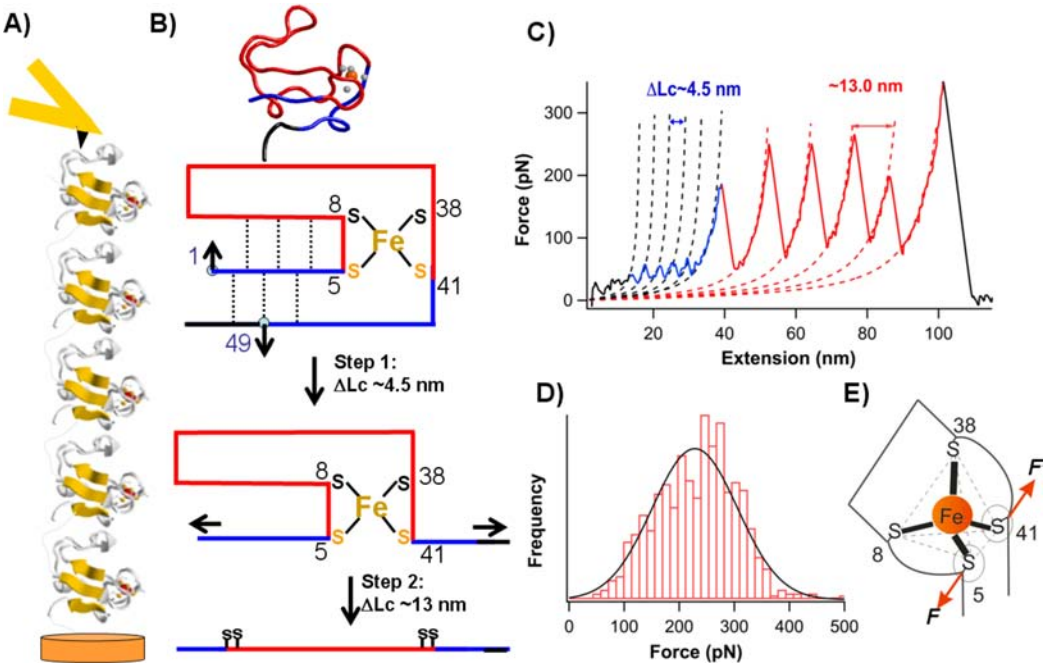

Figure 2. Mechanical stability of FeS_4 stretched from Fe−S(Cys5) and Fe−S(Cys41) in RD1,49. (A) Schematic of the mechanical unfolding experiment on RD1,49 by AFM. (B) The two-step unfolding of rubredoxin when it is stretched from residue 1 and 49. The first step corresponds to the mechanical unfolding of structures (in blue) outside the FeS_4 center, while the second step corresponds to the rupture of the FeS_4 center and subsequent stretching of the residues (in red) that are originally sequestered by the FeS_4 center. Sulfur atoms colored in orange indicate those in the anchoring cysteine residues. Black line indicates regions of the protein that are outside of the points of force application and are thus not part of the extensible polypeptide. This coloring scheme is used for all figures in this study. Top panel: 3D structure representation of RD1,49; bottom panel: line drawing schematic. Both panels use the same coloring scheme. C) The typical force extension curve from the mechanical unfolding of RD1,49 showing two different types of force peaks. Low force peaks at the beginning arise from the unfolding of residues before the FeS_4 center (colored in blue), leading to a $\Delta L_c \sim 4.5$ nm. The rupture of the FeS_4 center and the extension of previously buried residues (colored in red) give rise to high force peaks with a $\Delta L_c \sim 13$ nm. Dotted lines are WLC fits to the unfolding events with a persistence length of 0.4 nm. (D) A histogram of rupture force for the FeS_4 center with an average value of 227 ± 79 pN (n = 1063). Solid line is the Gaussian fit to the data. (E) A schematics shows how the tetrahedron FeS_4 center is stretched in RD1,49 via anchoring ferric−thiolate bonds Fe−S(Cys5) and Fe−S(Cys41).

measurements were done on polyproteins at a constant velocity, the force evolves in a complex manner in the sawtooth-like force−extension curves, making it difficult to derive analytical solutions for the relationship between the rupture force and pulling velocity.[39,40] Thus we used well-established Monte Carlo simulations procedures[35,41] to estimate the dissociation rate constant k_{r0} at zero force and Δx by including similar experimental conditions. Briefly, in such Monte Carlo simulations, we stretch a virtual polypeptide made of folded rubredoxin domains of an initial contour length of 30 nm at a certain pulling speed from zero extension. The persistence length of the unfolded polypeptide chain is taken as 0.4 nm. The contour length of the polyprotein chain will change upon the unfolding of rubredoxin domains. In every time step (typically 0.1 ms), the extension x is increased, and the entropic force acting on the polyprotein chain at the current extension x is then calculated using the interpolation formula of WLC model of polymer elasticity:[33] $F(x) = (k_BT/p)\cdot(x/L + 0.25\cdot(1 - x/L)^{-2} - 0.25)$. The probability of observing the rupture of any FeS_4 center in rubredoxin was calculated using the following equation: $Pu = N_f k_r(F)\cdot\Delta t$, where Pu is the rupture probability of any FeS_4 center, N_f is the number of folded rubredoxin domains, $k_r(F)$ is the force-dependent rate constant of the FeS_4 center, and Δt is polling time interval. Then each domain was polled to determine the status of the FeS_4 center,[35] following the Monte Carlo approach. Based on this method, force−extension curves for different rubredoxin polyproteins were generated (typically ∼100 runs), and the average rupture force at each pulling speed was calculated and compared with experimental values.[35]

RESULTS

Design Principle for Probing Mechanical Anisotropy of the FeS_4 Center. The first step in exploring the molecular mechanical anisotropy of the FeS_4 center is choosing residues, or anchoring points, at which the stretching force can be applied to the FeS_4 cluster along the polyprotein rope. Thanks to the simple structure of the metal center, the four ferric−thiolate bonds naturally allow the metal center to be stretched in different directions. Thus, selecting different combinations of the two individual ferric−thiolate bonds enables us to fully explore the mechanical anisotropy of the target. Based on the structure of the FeS_4 center in the protein, four different bond combinations were chosen: Fe−S(Cys5)/Fe−S(Cys41), Fe−S(Cys8)/Fe−S(Cys41), Fe−S(Cys8)/Fe−S(Cys38), and Fe−S(Cys5)/Fe−S(Cys38).

The FeS_4 center is covalently enclosed in the protein structure, making it challenging to directly apply the stretching force to the metal center along different directions. Since the stretching force is transmitted from one anchoring point to the other through the polypeptide chain, we can use the polypeptide chain of rubredoxin as a handle to apply force to the FeS_4 center along a defined pulling direction. For example, stretching rubredoxin along its N- to C-termini will first lead to the unfolding of structural elements that are outside of the FeS_4 center (blue residues in Figure 1B), then the stretching force can be applied to the FeS_4 center via Cys5 and Cys41, thus defining the direction along which the FeS_4 center is stretched.

dx.doi.org/10.1021/ja406695g | J. Am. Chem. Soc. 2013, 135, 17783−17792

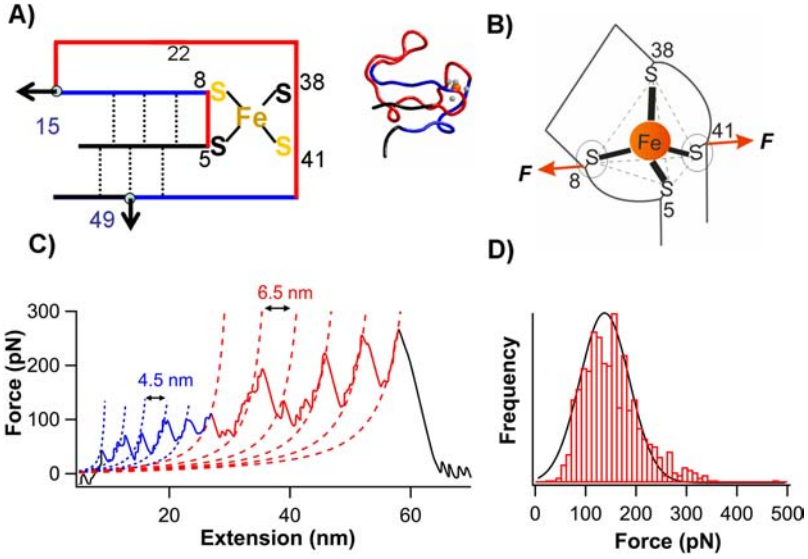

Figure 3. Mechanical stability of FeS_4 as it is stretched across Fe−S(Cys8) and Fe−S(Cys41).A) Schematic showing the stretching scenario of RD15,49. Left panel: line drawing schematic; right panel: 3D structure with the same coloring scheme. The mechanical unfolding of RD15,49 occurs in two steps: sequences colored in blue are ruptured and extended first, followed by the mechanical rupture of the FeS_4 center, and the extension of residues colored in red. Black lines indicate regions of the protein that are outside of the points of force application and are thus not part of the extensible polypeptide. (B) A schematics shows how the tetrahedron FeS_4 center is stretched in RD15,49 via anchoring ferric−thiolate bonds Fe−S(Cys8) and Fe−S(Cys41)s. (C) A typical force extension curve of mechanical unfolding of RD15,49 shows a two-step unfolding scenario. The unfolding and extension of sequences colored in blue results in force peaks of ΔL_c of ∼4.5 nm, while the rupture of the FeS_4 center results in force peaks of ΔL_c of ∼6.5 nm. Dotted lines are WLC fits to the experimental data with a persistence length of 0.4 nm. (D) A histogram of rupture force of the FeS_4 center with an average value of 152 ± 60 pN (n = 708). Solid line is a Gaussian fit to the experimental data.

Using similar strategies, we can stretch the FeS_4 center along the other three distinct directions. To do so, we adapted a cysteine tether approach, which has been used extensively in investigating the mechanical anisotropy of proteins,[4,5,7,8] to investigate the molecular level mechanical anisotropy of the FeS_4 center. In this strategy, a pair of residues outside the metal center in rubredoxin are mutated to cysteines, which serve as the anchoring points for the stretching force to be applied to different part of rubredoxin and eventually to the FeS_4 center along different directions[17] (Supporting Information) (Figure 2). In addition, stretching rubredoxin along the direction set by these two exogenous cysteine residues forces rubredoxin to unfold in a specific pathway, giving rise to a specific contour length increment upon the rupture of the FeS_4 center and subsequent unfolding of rubredoxin.[17] Such specific contour length increments allow for unambiguous identification of the metal cluster rupture events during single molecule stretching experiments.

Following this design principle, we engineered four different bicysteine rubredoxin variants. Individual variants were chemically linked through the two engineered cysteines through a maleimide−thiol coupling reaction, resulting in a polyprotein $(RD\text{-variant})_n$ composed of identical tandem repeats of the rubredoxin variant with specific linkages. These introduced cysteine residues serve as the anchoring sites, where force used to ultimately unfold the metal center will be applied.

Mechanical Anisotropy of the FeS_4 Center at the Single Bond Level. We first stretched the FeS_4 center along the direction of Fe−S(Cys5) and Fe−S(Cys41) bonds using RD1,49 variant. Stretching the $(RD1,49)_n$ polyprotein results in characteristic sawtooth-like force−extension curves resulted from unfolding of rubredoxin.[17,28] Fitting the force−extension trace using the WLC model of polymer elasticity[33] reveals force peaks with two different contour length increments (ΔL_c): ∼4.5 and ∼13.0 nm (Figure S1). This result supports a two-step unfolding scenario for RD1,49 (Figure 2B). Residues 1−4 and 42−49, located outside the metal center, unfold first at ∼62 pN (Figure S1A, Table S1), and their extension leads to force peaks with a ΔL_c of 4.4 ± 1.0 nm (Figure S1B) (colored in blue in Figure 2), which is close to the expected value of 3.95 nm (12aa*0.365 nm/aa + 0.65 nm − 1.08 nm = 3.95 nm, where 0.365 nm/aa is the length per amino acid,[42] 0.65 nm is the through space distance between Cys5 and Cys41, and 1.08 nm is the through space distance between residues 1 and 49 in folded rubredoxin). The subsequent rupture of the FeS_4 center leads to force peaks with a ΔL_c of 13.0 ± 0.8 nm (colored in red in Figure 2), close to the expected contour length increment (37aa (residues 5−41)*0.365 nm/aa − 0.65 nm = 12.9 nm, where 0.65 nm is the through space distance between Cys5 and Cys41). Thus, the 227 ± 79 pN (n = 1063) force arising from peaks with a ΔL_c of ∼13 nm can be unambiguously assigned as the rupture force of the FeS_4 center as it is stretched across Fe−S(Cys5) and Fe−S(Cys41) bonds.

The rupture of FeS_4 center was then investigated as force is applied through Fe−S(Cys8) and Fe−S(Cys41) bonds within the $(RD15,49)_n$ polyprotein (Figures 3A,B and S2). Similar to the two-step unfolding scenario observed for RD1,49, the AFM results from RD15,49 show that RD15−49 also unfolds in a two-step manner (Figures 3C and S2A). The first step corresponds to the rupture and extension of the protein structure outside the metal cluster (residues 49−41) as well as the alignment of residues 8−15 (colored in blue) and results in force peaks with an average unfolding force of 85 ± 30 pN (Figure S2B) and a ΔL_c of 4.5 ± 0.8 nm (Figure S2C), which is close to the expected value of 4.6 nm ((8 + 9)aa*0.365 nm/aa − 1.62 nm, where 1.62 nm is the through space distance between residues 15 and 49) (Figure S2). After the rupture of these secondary structures, the stretching force will be applied

dx.doi.org/10.1021/ja406695g | J. Am. Chem. Soc. 2013, 135, 17783−17792

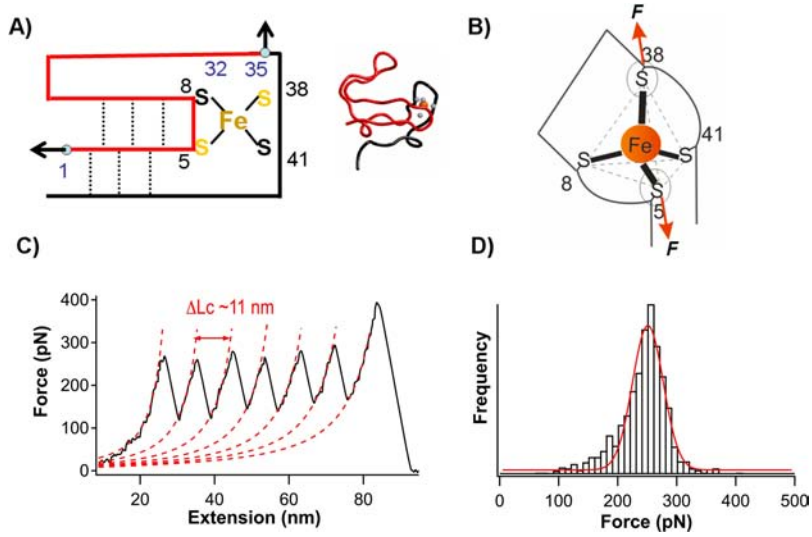

Figure 4. Mechanical stability of FeS_4 as it is stretched from Fe−S(Cys5) and Fe−S(Cys8). (A) Schematic showing the stretching scenario of RD1,35. Left panel: line drawing schematic; right panel: 3D structure representation with the same coloring scheme. Upon mechanical rupture of the FeS_4 center, structural elements colored in red will be extended and contribute to the observed ΔL_c, while sequences colored in black do not contribute to ΔL_c. (B) A schematics shows how the tetrahedron FeS_4 center is stretched in RD1,35 via anchoring ferric−thiolate bonds Fe−S(Cys5) and Fe−S(Cys38). (C) A typical force extension curve from the mechanical unfolding of RD1,35 shows force peaks with a ΔL_c of ∼11 nm, which arise from the rupture of the FeS_4 center and unfolding of rubredoxin. (D) A histogram of rupture force shows an average unfolding force of 242 ± 40 pN (n = 1340). Solid line is the Gaussian fit to the experimental data.

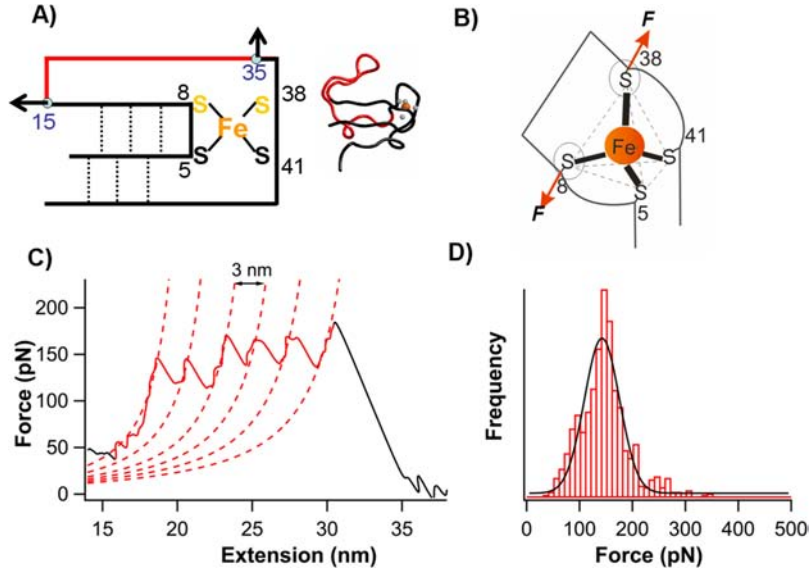

Figure 5. Mechanical stability of FeS_4 as it is stretched from Fe−S(Cys8) and Fe−S(Cys38). (A) Schematic showing how RD15,35 is stretched. Left panel: line drawing schematic; right panel: 3D structure representation with the same coloring scheme. (B) A schematics shows how the tetrahedron FeS_4 center is stretched in RD15,35 via anchoring ferric−thiolate bonds Fe−S(Cys8) and Fe−S(Cys38. (C) A typical force extension curve from the mechanical unfolding of RD15,35. The rupture of FeS_4 center and unfolding of rubredoxin result in force peaks with a ΔL_c of ∼3 nm. Dotted lines are WLC fits to the data. (D) Histogram of the rupture force shows an average value of 146 ± 49 pN (n = 985). Solid line is the Gaussian fit to the data.

to the metal cluster directly via the Fe−S(Cys8) and Fe−S(Cys41) bonds. Rupture of the FeS_4 cluster results in a force peak with a ΔL_c of 6.4 ± 0.7 nm (Figure S2C). The average rupture force of the FeS_4 cluster along the Fe−S(Cys8) and Fe−S(Cys41) direction is 152 ± 60 pN (n = 708) (Figure 3D), which is less than that observed along the Fe−S(Cys5) and Fe−S(Cys41) direction of RD1,49. This result clearly indicates that the stability of the FeS_4 center varies considerably when stretched from different directions, providing experimental evidence for the mechanical anisotropy of FeS_4 center in rubredoxin.

Following similar strategies, we also measured the mechanical stability of the FeS_4 cluster along two additional pulling directions (Fe−S(Cys38)−Fe-S(Cys8); Fe−S(Cys5)- Fe−S-(Cys38)) using rubredoxin variants $(RD15,35)_n$ and $(RD1,35)_n$.

Stretching the metal center from Fe−S(Cys5) to Fe−S(Cys38) is achieved using RD1,35 (Figures 4 and S3). Stretching RD1,35 results in an one-step rupture of the FeS_4

dx.doi.org/10.1021/ja406695g | J. Am. Chem. Soc. 2013, 135, 17783−17792

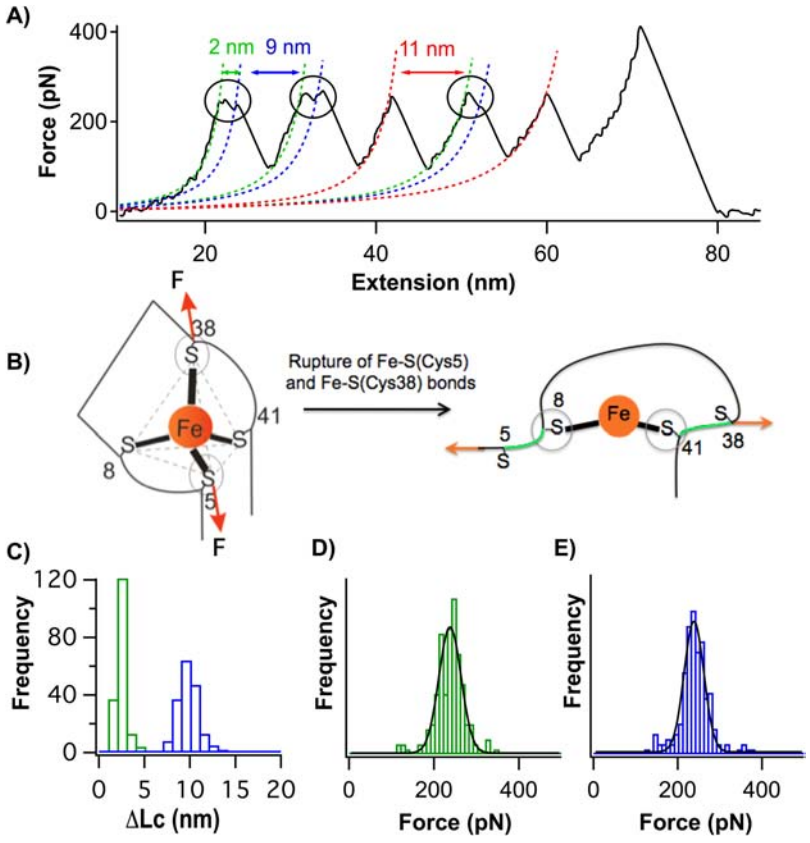

Figure 6. The mechanical rupture of the FeS_4 center can occur in a stepwise fashion when it is stretched from Cys5-Fe-Cys38 direction. (A) A typical force−extension curve reveals a two-step rupture mechanism. Circled force peaks are clearly resolvable twin peaks with ΔL_c of ∼2 and 9 nm, respectively. (B) A simple schematics of FeS_4 shows how Fe−S(Cys8) and Fe−S(Cys38) bonds are stretched after Fe−S(Cys5) and Fe−S(Cys38) bonds are ruptured, which leads to the extension of six residues (colored in green). Sulfur atoms in the anchoring ferric−thiolate bonds are circled. (C) ΔL_c histogram of the twin force peaks. The first peak is with a ΔL_c of 1.9 ± 0.3 nm (green), and the second peak is with ΔL_c of 9.0 ± 0.3 nm (blue). (D,E) Histogram of the rupture forces from peaks with a ΔL_c = 1.9 ± 0.3 nm (D) and ΔL_c = 9.0 ± 0.3 nm (E). The average rupture force for the two rupture steps is 235 ± 35 pN (n = 173) and 239 ± 38pN (n = 173), respectively.

cluster and subsequent unfolding of rubredoxin, giving rise to force peaks of ΔL_c of 11.1 ± 1.2 nm, which result from the rupture of the FeS_4 center and subsequent extension of residues 5−35 (Figure S3). The rupture force measured along the direction of Cys5-Fe-Cys38 is 242 ± 40 pN (n = 1340) (Figure 4D). Similarly, the mechanical rupture of the FeS_4 cluster along the direction of Cys8-Fe-Cys38 using RD15,35 also follows an one-step mechanism (with a ΔL_c of ∼2.7 ± 0.4 nm), giving an average mechanical rupture force of 146 ± 49 (n = 985) (Figures 5 and S4).

From these results, it is evident that the very small molecular object FeS_4 cluster exhibits strong mechanical anisotropy when stretched. In particular, the metal cluster is most resistant along the pulling direction of Cys5-Fe-Cys38 at the given pulling velocity of 400 nm/s.

Mechanical Rupture Mechanisms of the FeS_4 Center When Stretched from Cys5 to Cys38. Due to the limited length resolution of the AFM in stretching flexible polymers and the small length gain upon the rupture of a single ferric−thiolate bond in the FeS_4 center in rubredoxin, it has been difficult to discern the detailed mechanical rupture mechanism of the FeS_4 center. Using a loop elongation variant of rubredoxin, we have shown that the mechanical rupture of the FeS_4 center follows a stochastic mechanism involving concurrent rupture of multiple ferric−thiolate bonds as well as a stepwise rupture mechanism with the concurrent rupture mechanism being dominant.[23] However, such mechanisms are yet to be confirmed in wild-type rubredoxin.

A close analysis of the force peaks in the force−extension curves of RD1,35 provides valuable insights into the mechanical rupture mechanism of the FeS_4 center in wild-type rubredoxin. We found that the majority of mechanical rupture events of the FeS_4 center in RD1,35 occurs in a single step fashion and results in a single force peak, suggesting that the rupture of the FeS_4 center involves concurrent rupture of multiple ferric−thiolate bonds. In addition, a small population (∼10%) of rupture events of the FeS_4 center appears to occur in a two-step fashion (Figure 6A,B), resulting in clearly resolvable twin force peaks (circled in Figure 6A, also see Figure S6). The first step results in a rupture event with a ΔL_c of ∼2 nm, and the second step results in a rupture event with a ΔL_c of ∼9 nm, with the sum of the two ΔL_c being 11 nm, which agrees well with the ΔL_c observed for the one-step rupture of the FeS_4 center (Figure 4). Fitting the twin peaks using WLC model with the same persistence length[43] yields ΔL_{c1} of 1.9 ± 0.3 nm and ΔL_{c2} of 9.0 ± 0.3 nm (Figure 6C). The corresponding force value for the twin force peaks is 235 ± 35 pN (n = 177) and 239 ± 38pN (n = 173), respectively (Figure 6D,E). This first step (ΔL_c of ∼2 nm) is likely due to the rupture of Fe−S(Cys5) and Fe−S(Cys38) thiolate bonds (with Fe−S(Cys8) and Fe−S(Cys41) remain intact) and the subsequent extension of residues 5−8 and 38−41 (6aa*0.365 nm/aa). The second step (ΔL_c of 9

dx.doi.org/10.1021/ja406695g | J. Am. Chem. Soc. 2013, 135, 17783−17792

nm) thus corresponds to the rupture of Fe−S(Cys8) and Fe−S(Cys41) bonds and subsequent unfolding and extension of residues 8−41 (Figure 6B). This result strongly indicates that the rupture of these FeS_4 centers occurs via a stepwise rupture mechanism.[44] These results are in excellent agreement with our previous findings on a loop-elongation variant of rubredoxin,[23] corroborating that the mechanical rupture of the FeS_4 center follows multiple, complex pathways that include concurrent rupture of multiple ferric−thiolate bonds as well as sequential rupture of ferric−thiolate bonds.[23]

FeS_4 Cluster Exhibits Distinct Kinetic Properties along Different Pulling Directions. To investigate how different pulling geometries affect the mechanical rupture kinetics of the FeS_4 center, we carried out experiments at different pulling speeds on all four RD mutants to measure the dependence of the rupture force on the pulling speeds. The speed dependency of mechanical rupture force of the FeS_4 center along different pulling directions is shown in Figure 7. It is evident that the same FeS_4 center exhibits distinct kinetic properties depending on the pulling directions. The spontaneous rupture rate constant k_r and the distance between the bound state and mechanical rupture transition state Δx for these different scenarios were estimated using well-established Monte Carlo simulations procedures (Table 1).[41]

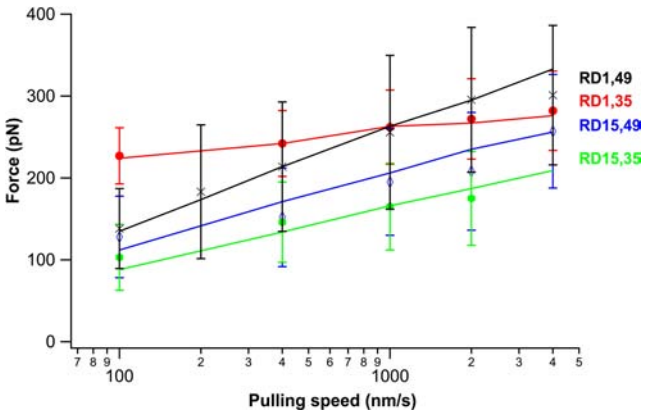

Figure 7. The mechanical stability of the FeS_4 center displays distinct pulling speed dependencies as it is pulled along different pulling directions. Solid lines are Monte Carlo simulation results using k_{r0} and Δx that are tabulated in Table 1.

CXXC Chelation Loops Offer Additional Pulling Geometry. The FeS_4 center in rubredoxin is a highly cooperative structure.[23,45,46] In the four pulling geometries we have investigated, the metal center is always stretched by subjecting two ferric−thiolate bonds to the stretching force. The FeS_4 center in rubredoxin is constituted by two CXXC chelation loops such that the two neighboring cysteinyl ligands (Cys5- and Cys8- or Cys38- and Cys41) are connected by the CXXC loops, which is different from synthetic inorganic FeS_4 analogues (in which the cysteinyl ligands are monodentate). This unique arrangement provides additional possible geometries for probing the mechanical resistance of the FeS_4 center in *pf*-rubredoxin (Figure 8A,B). Mutating residues 6 and 40 inside the chelation loops to cysteines enabled us to mechanically stretch the FeS_4 center along a unique direction such that ferric−thiolate bonds Fe−S(Cys5) and Fe−S(Cys8) bear the stretching force simultaneously on the side of the C5XXC8 loop while Fe−S(Cys38) and Fe−S(Cys41) bonds bear the load on the C38XXC41 loop side simultaneously, due to the fact that the two anchoring residues are in the middle of the two CXXC loops, respectively. This pulling geometry will likely offer much higher mechanical resistance for the FeS_4 center when compared to the other four possible pulling geometries, since the four ferric−thiolate bonds will be subject to the stretching force simultaneously.

To experimentally investigate this possibility, we designed bicysteine variant RD6,40. Stretching the $(RD6,40)_n$ polyprotein results in sawtooth-like force−extension curves with a contour length increment ΔL_c of 12.5 nm (Figures 8C and S5), resulting from the rupture of the FeS_4 center and subsequent unfolding of rubredoxin. As anticipated, the mechanical rupture force of 327 ± 137 pN (n = 130) is much higher than that exhibited by other pulling geometries. In fact, this rupture force almost doubles that observed for RD15,35 where the FeS_4 center is ruptured along the direction of Fe−S(Cys8)−Fe-S(Cys38). This suggests that loading four ferric thiolate bonds directly and simultaneously offers the highest mechanical stability for the FeS_4 center.

Table 1. Mechanical Stability and Rupture Kinetics of the FeS_4 Metal Center in *pf*-Rubredoxin in Different Pulling Geometries[a]

protein	F_r (pN) (average ± stdv)	k_r (s^{-1})	Δx (nm)
01,49	227 ± 79	0.15	0.11
15,49	152 ± 60	0.6	0.15
15,35	146 ± 49	0.7	0.18
01,35	242 ± 40	3×10^{-6}	0.30

[a] F_r: mechanical rupture force at the pulling speed of 400 nm/s; k_{r0}: spontaneous dissociation rate of the FeS_4 center; Δx: distance between the bound state and the mechanical rupture transition state. The error of the estimated Δx is ∼10%, and k_{r0} is typically accurate within a factor of 3.

DISCUSSION

The Molecular-Scale FeS_4 Cluster Exhibits Mechanical Anisotropy. By stretching the FeS_4 center from four different directions using single molecule AFM, we discovered that the mechanical stability of the metal center is depended on the direction of the applied force. The rupture force of the FeS_4 cluster measured from different pulling directions ranges from ∼150 to ∼250 pN at a pulling speed of 400 nm/s. Compared with macromolecules such as proteins, the very small and simple FeS_4 center studied here exhibits considerable mechanical anisotropy. Our results suggest that this mechanical anisotropy may be a universal feature for any asymmetrical 3D structure, even down to a molecular scale. In addition, the mechanical rupture of the FeS_4 center exhibits different rupture kinetics and mechanism when the FeS_4 center is stretched along different directions. This observation suggests that such mechanical anisotropy can be potentially useful in controlling the mechanochemical reactivity of metal centers as well as other small molecular objects.

Furthermore, the metal center motif is a critical part of metalloproteins.[14,15] Besides their functional roles, metal centers can play important structural roles in the (un)folding and stability of metalloproteins. For example, metal centers mediated by iron and zinc play important structural roles for iron−sulfur proteins and zinc-finger proteins.[47−49] Thus, from the perspective of metalloproteins, the knowledge of stability of metal centers is important for understanding how metal-

dx.doi.org/10.1021/ja406695g | J. Am. Chem. Soc. 2013, 135, 17783−17792

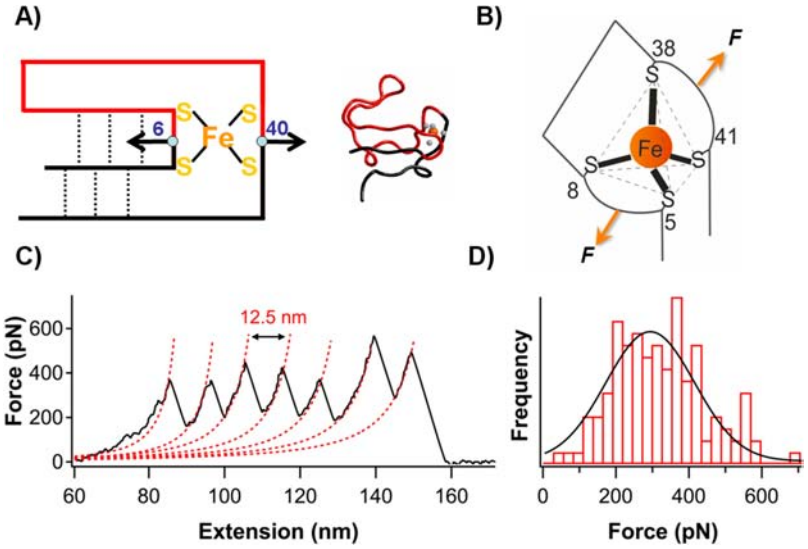

Figure 8. Mechanical stability of FeS_4 being stretched from Cys6 and Cys40. (A) Schematic showing the stretching scenario of RD6,40. Left panel: line drawing schematic; right panel: 3D structure representation with the same coloring scheme. (B) A simple structure of FeS_4 showing that all four Fe−S bond are initially stretched. (C) Typical force extension curves from the mechanical unfolding of RD6,40 shows force peaks with a ΔL_c ~12.5 nm. (D) The histogram of rupture force demonstrating an average value of 327 ± 137 pN (n = 130). Solid line is a Gaussian fit to the data.

loproteins work. The single molecule force spectroscopy method demonstrated here could allow for the investigation of whether the mechanical anisotropy of metal centers in metalloproteins has any biological implications in their natural settings.

It is also important to point out that, upon stretching from different directions, the rubredoxin protein framework also exhibits clear mechanical anisotropy, although protein's mechanical anisotropy is not the focus of this study. For example, upon stretching from its N−C-termini, structural elements outside of the FeS_4 center unfolds at forces that are below our detection limit, no unfolding force peaks were observed.[17] In contrast, stretching rubredoxin via residue 1 and 49 results in clear unfolding force peaks of the structural elements outside of the FeS_4 center (ΔL_c of ~4.5 nm and unfolding force of ~60 pN (Figure 2 and Figure S1). Thus, rubredoxin is a great example combining the mechanical anisotropy at the protein level as well as the level of the metal center.

Molecular Origin of Mechanical Anisotropy in the FeS_4 Cluster in Rubredoxin. The FeS_4 cluster consists of five atoms with four corresponding ferric−thiolate bonds arranged into a tetrahedron. Depending on which two ligands are stretched, the FeS_4 cluster can be stretched along six distinct pulling directions. If the four cysteinyl ligands are identical (such as the chemically synthesized analogue $Fe(SPh)_4$), the FeS_4 cluster will have a T_d symmetry.[19] Therefore, all six pulling directions should be equivalent due to the structural symmetry of the tetrahedron. Such molecular objects should be mechanically isotropic.

For the FeS_4 cluster in rubredoxin, all four ligands are cysteines; thus the cluster itself has high symmetry, raising the question as to why the FeS_4 in rubredoxin is not mechanically isotropic. To address this question, the influence of the rubredoxin protein framework on the FeS_4 center should be taken into account. On the one hand, the two CXXC chelation loops in rubredoxin are different, and amide backbone hydrogen bonds from secondary coordination sphere modify the ferric−thiolate bonds to different extents.[18,23,50−53] On the other hand, the degree of solvent exposure is different for different sides of the FeS_4. For example, Cys8 and Cys41 are more solvent exposed than Cys5 and Cys38.[50,54,55] All these effects lead to a distorted tetrahedral geometry of the FeS_4 center in rubredoxin and render an asymmetric protein environment for the FeS_4 center.[19,22] The distorted tetrahedral geometry of the FeS_4 center has been demonstrated by X-ray and NMR studies, which have shown slightly different ferric−thiolate bond length.[22,50,56] Such molecular asymmetry likely underpins the observed molecular mechanical anisotropy for the FeS_4 center in rubredoxin. Furthermore, when pulled from different directions in our experimental design, different portions of rubredoxin are ruptured. The partial unfolding of rubredoxin likely changes the local environment of the FeS_4 cluster, including the degree of solvent exposure. It is likely that mechanical anisotropy arises from structural asymmetry in the FeS_4 cluster and the modulation of the local environment due to partial unfolding of rubredoxin. Detailed computational studies, as those recently carried out for wild-type rubredoxin,[24] should provide further insights into the contribution of these mechanisms and how different molecular interactions define mechanical anisotropy.

■ CONCLUSION

Combining protein engineering and single molecule AFM techniques, we have stretched and ruptured the FeS_4 metal center in rubredoxin along five distinct pulling directions. In these experiments, the protein structure of rubredoxin serves as an indispensible signature for identifying the mechanical rupture of the FeS_4 center. Our results showed that the mechanical stability and rupture mechanism of this small FeS_4 center, which consists of only four ferric thiolate bonds, strongly depend on the pulling direction along which it is stretched, suggesting considerable mechanical anisotropy for this small molecular object. Such mechanical anisotropy likely originates from the structural asymmetry of the metal center and the influence caused by the local protein environment. Our study extends the concept of mechanical anisotropy to the molecular level and suggests that mechanical anisotropy may be

dx.doi.org/10.1021/ja406695g | J. Am. Chem. Soc. 2013, 135, 17783−17792

a universal feature for any asymmetrical 3D structure, from macroscopic scale down to molecular scale.

■ ASSOCIATED CONTENT

Supporting Information

Pulling direction versus effective mechano-reaction coordinate; signatures of mechanical rupture of the FeS_4 center and mechanical unfolding of *pf*-rubredoxin in different pulling geometries; mechanical unfolding signatures of RD1,49; mechanical rupture of the FeS_4 center in RD15,49 via force-bearing bonds Fe−S(Cys5) and Fe−S(Cys41); mechanical rupture of the FeS_4 center via force-bearing bonds Fe−S(Cys5) and Fe−S(Cys35) in RD1,35; mechanical rupture of the FeS_4 center via force-bearing bonds Fe−S(Cys8) and Fe−S(Cys38) in RD15,35; mechanical rupture of the FeS_4 center via anchoring residues 6 and 40; differences between the single-step and two-step rupture events of FeS_4 center in RD1,35. This material is available free of charge via the Internet at http://pubs.acs.org.

■ AUTHOR INFORMATION

Corresponding Author

Hongbin@chem.ubc.ca

Notes

The authors declare no competing financial interest.

■ ACKNOWLEDGMENTS

We thank Ashlee Jollymore for critical reading of the manuscript. This work is supported by the Natural Sciences and Engineering Research Council of Canada (NSERC), Canada Research Chairs Program and Canada Foundation for Innovation.

■ REFERENCES

(1) Owen, A. J.; Ward, I. M. *J. Macro. Sci. B* **1973**, *7*, 417.
(2) Ward, I. M.; Sweeney, J. In *Mechanical Properties of Solid Polymers*; John Wiley & Sons, Ltd: Chichester, U.K., 2012, p 167.
(3) Carrion-Vazquez, M.; Li, H.; Lu, H.; Marszalek, P. E.; Oberhauser, A. F.; Fernandez, J. M. *Nat. Struct. Biol.* **2003**, *10*, 738.
(4) Dietz, H.; Berkemeier, F.; Bertz, M.; Rief, M. *Proc. Natl. Acad. Sci. U.S.A.* **2006**, *103*, 12724.
(5) Li, Yongnan D.; Lamour, G.; Gsponer, J.; Zheng, P.; Li, H. *Biophys. J.* **2012**, *103*, 2361.
(6) Brockwell, D. J.; Paci, E.; Zinober, R. C.; Beddard, G. S.; Olmsted, P. D.; Smith, D. A.; Perham, R. N.; Radford, S. E. *Nat. Struct. Mol. Biol.* **2003**, *10*, 731.
(7) Lee, W.; Zeng, X.; Rotolo, K.; Yang, M.; Schofield, C. J.; Bennett, V.; Yang, W.; Marszalek, P. E. *Biophys. J.* **2012**, *102*, 1118.
(8) Schlierf, M.; Rief, M. *Angew. Chem., Int. Ed. Engl.* **2009**, *48*, 820.
(9) Yang, G.; Cecconi, C.; Baase, W. A.; Vetter, I. R.; Breyer, W. A.; Haack, J. A.; Matthews, B. W.; Dahlquist, F. W.; Bustamante, C. *Proc. Natl. Acad. Sci. U.S.A.* **2000**, *97*, 139.
(10) Graham, T. G. W.; Best, R. B. *J. Phys. Chem. B* **2011**, *115*, 1546.
(11) Junker, J. P.; Rief, M. *Angew. Chem., Int. Ed. Engl.* **2010**, *49*, 3306.
(12) Jagannathan, B.; Elms, P. J.; Bustamante, C.; Marqusee, S. *Proc. Natl. Acad. Sci. U.S.A.* **2012**, *109*, 17820.
(13) Gao, Y.; Sirinakis, G.; Zhang, Y. L. *J. Am. Chem. Soc.* **2011**, *133*, 12749.
(14) Holm, R. H.; Kennepohl, P.; Solomon, E. I. *Chem. Rev.* **1996**, *96*, 2239.
(15) Bertini, I.; Gray, H. B.; Lippard, S. J.; Valentine, J. S. *Bioinorganic Chemistry*; University Science Books: Mill Valley, CA, 1994.
(16) Blake, P. R.; Park, J. B.; Bryant, F. O.; Aono, S.; Magnuson, J. K.; Eccleston, E.; Howard, J. B.; Summers, M. F.; Adams, M. W. *Biochemistry* **1991**, *30*, 10885.
(17) Zheng, P.; Li, H. *J. Am. Chem. Soc.* **2011**, *133*, 6791.
(18) Zheng, P.; Takayama, S.-i. J.; Mauk, A. G.; Li, H. *J. Am. Chem. Soc.* **2012**, *134*, 4124.
(19) Lane, R. W.; Ibers, J. A.; Frankel, R. B.; Holm, R. H. *Proc. Natl. Acad. Sci. U.S.A.* **1975**, *72*, 2868.
(20) Lane, R. W.; Ibers, J. A.; Frankel, R. B.; Papaefthymiou, G. C.; Holm, R. H. *J. Am. Chem. Soc.* **1977**, *99*, 84.
(21) Averill, B. A.; Bale, J. R.; Ormejohnson, W. H. *J. Am. Chem. Soc.* **1978**, *100*, 3034.
(22) Day, M. W.; Hsu, B. T.; Joshuator, L.; Park, J. B.; Zhou, Z. H.; Adams, M. W. W.; Rees, D. C. *Protein Sci.* **1992**, *1*, 1494.
(23) Zheng, P.; Takayama, S.-i. J.; Mauk, A. G.; Li, H. *J. Am. Chem. Soc.* **2013**, *135*, 7992.
(24) Arantes, G. M.; Bhattacharjee, A.; Field, M. J. *Angew. Chem., Int. Ed. Engl.* **2013**, *52*, 8144.
(25) Fernandez, J. M.; Li, H. *Science* **2004**, *303*, 1674.
(26) Hutter, J. L.; Bechhoefer, J. *Rev. Sci. Instrum.* **1993**, *64*, 1868.
(27) Rief, M.; Gautel, M.; Oesterhelt, F.; Fernandez, J. M.; Gaub, H. E. *Science* **1997**, *276*, 1109.
(28) Carrion-Vazquez, M.; Oberhauser, A. F.; Fisher, T. E.; Marszalek, P. E.; Li, H.; Fernandez, J. M. *Prog. Biophys. Mol. Biol.* **2000**, *74*, 63.
(29) Dietz, H.; Bertz, M.; Schlierf, M.; Berkemeier, F.; Bornschlogl, T.; Junker, J. P.; Rief, M. *Nat. Protoc.* **2006**, *1*, 80.
(30) Brockwell, D. J. *Curr. Nanosci.* **2007**, *3*, 3.
(31) Li, H. *Protein Nanomechanics*; Academic Press: Oxford, 2011; Vol. 2.
(32) Marszalek, P. E.; Dufrene, Y. F. *Chem. Soc. Rev.* **2012**, *41*, 3523.
(33) Marko, J. F.; Siggia, E. D. *Macromolecules* **1995**, *28*, 8759.
(34) Carrion-Vazquez, M.; Oberhauser, A. F.; Fowler, S. B.; Marszalek, P. E.; Broedel, S. E.; Clarke, J.; Fernandez, J. M. *Proc. Natl. Acad. Sci. U.S.A.* **1999**, *96*, 3694.
(35) Oberhauser, A. F.; Marszalek, P. E.; Erickson, H. P.; Fernandez, J. M. *Nature* **1998**, *393*, 181.
(36) Bell, G. I. *Science* **1978**, *200*, 618.
(37) Evans, E. *Annu. Rev. Biophys. Biomol. Struct.* **2001**, *30*, 105.
(38) Evans, E.; Ritchie, K. *Biophys. J.* **1997**, *72*, 1541.
(39) Schlierf, M.; Li, H.; Fernandez, J. M. *Proc. Natl. Acad. Sci. U.S.A.* **2004**, *101*, 7299.
(40) Cao, Y.; Li, H. *Langmuir* **2011**, *27*, 1440.
(41) Rief, M.; Fernandez, J. M.; Gaub, H. E. *Phys. Rev. Lett.* **1998**, *81*, 4764.
(42) Dietz, H.; Rief, M. *Proc. Natl. Acad. Sci. U.S.A.* **2006**, *103*, 1244.
(43) It is of note that although the number of data points in the second peak of the twin peaks is limited, we can use WLC fits to readily estimate the contour length increment during the first rupture event in the twin peak. Similar scenarios were also observed and treated in the mechanical unfolding of proteins, where unfolding intermediate states only have marginal kinetic stability or have short contour length increment (refs 57−59).
(44) It is important to note that current AFM techniques cannot directly resolve length changes due to the rupture of a single ferric−thiolate bond in a soft polypeptide chain. The fact that we can resolve the stepwise rupture mechanism in RD1,35 benefits from the extension of six residues (residue 5−8 and 38−41) upon the rupture of ferric−thiolate bonds Fe−S(Cys5) and Fe−S(Cys38).
(45) Cavagnero, S.; Debe, D. A.; Zhou, Z. H.; Adams, M. W. W.; Chan, S. I. *Biochemistry* **1998**, *37*, 3369.
(46) Cavagnero, S.; Zhou, Z. H.; Adams, M. W.; Chan, S. I. *Biochemistry* **1998**, *37*, 3377.
(47) Wittung-Stafshede, P. *Acc. Chem. Res.* **2002**, *35*, 201.
(48) Johnson, D. C.; Dean, D. R.; Smith, A. D.; Johnson, M. K. *Annu. Rev. Biochem.* **2005**, *74*, 247.
(49) Lippard, S. J.; Berg, J. M. *Principles of bioinorganic chemistry*; University Science Books: Mill Valley, CA, 1994.

(50) Bau, R.; Rees, D. C.; Kurtz, D. M., Jr.; Scott, R. A.; Huang, H.; Adams, M. W. W.; Eidsness, M. K. *J. Biol. Inorg. Chem.* **1998**, *3*, 484.
(51) Zuris, J. A.; Halim, D. A.; Conlan, A. R.; Abresch, E. C.; Nechushtai, R.; Paddock, M. L.; Jennings, P. A. *J. Am. Chem. Soc.* **2010**, *132*, 13120.
(52) Lin, I. J.; Gebel, E. B.; Machonkin, T. E.; Westler, W. M.; Markley, J. L. *Proc. Natl. Acad. Sci. U.S.A.* **2005**, *102*, 14581.
(53) Gámiz-Hernández, A. P.; Galstyan, A. S.; Knapp, E.-W. *J. Chem. Theory Comput.* **2009**, *5*, 2898.
(54) Min, T.; Ergenekan, C. E.; Eidsness, M. K.; Ichiye, T.; Kang, C. *Protein Sci.* **2001**, *10*, 613.
(55) Sun, N.; Dey, A.; Xiao, Z. G.; Wedd, A. G.; Hodgson, K. O.; Hedman, B.; Solomon, E. I. *J. Am. Chem. Soc.* **2010**, *132*, 12639.
(56) Blake, P. R.; Park, J.-B.; Zhou, Z. H.; Hare, D. R.; Adams, M. W. W.; Summers, M. F. *Protein Sci.* **1992**, *1*, 1508.
(57) Dietz, H.; Rief, M. *Proc. Natl. Acad. Sci. U.S.A.* **2004**, *101*, 16192.
(58) Li, L.; Huang, H. H.; Badilla, C. L.; Fernandez, J. M. *J. Mol. Biol.* **2005**, *345*, 817.
(59) Bertz, M.; Rief, M. *J. Mol. Biol.* **2008**, *378*, 447.